Electronic Supplementary Information (SI) for

Anthracene based metal-organic framework showing efficient angle-dependent polarized emission, luminescent thermometry, and photoelectronic response

Ji-Rui Zhang,[ab] Hao-Yi Zhang[b], Jia-hui Guo[b], Zi-Han Liu[b], Cheng-Yu Ma[b], Xiao-Gang Yang,*[b] Xiao-Yan Lu,[b] Jian-Hua Qin,[b] and Lu-Fang Ma*[ab]

[a]College of Chemistry, Zhengzhou University, Zhengzhou 450001, P. R. China.

[b]College of Chemistry and Chemical Engineering, Luoyang Normal University, Henan Key Laboratory of Function-Oriented Porous Materials, Luoyang 471934, P. R. China.

*Corresponding author

Tel.: 86-379-68618328, Fax: 86-20-68618320.

E-mail: mazhuxp@126.com; yxg2233@126.com

1. Materials and general methods

All reagents were bought from commercial sources and used without any further purification. Power X-ray diffraction (PXRD) data was obtained using a Bruker D8-ADVANCE X-ray diffractometer with copper target (λ = 1.5418 Å) in a 2θ range from 5 to 50° at room temperature. The simulated PXRD data was calculated using Mercury 1.4.2 software based on single-crystal structures of **1**. Thermo gravimetric analysis (TGA) test was carried out on a SII EXSTAR6000 TG/DTA6300 thermal analysis system, ranging from room temperature to 800 ^{o}C under a nitrogen atmosphere at a ramping rate of 10 ^{o}C/min. FT-IR spectra was measured from 4000-400 cm^{-1} by employing the KBr pellet method. UV-Vis absorption spectra was recorded on S-3TECHCOMP spectrophotometer with a slit of 6 nm. Fluorescence spectra, fluorescence decay curve, temperature- and angle-dependent fluorescence emission were conducted on an Edinburgh FLS1000 fluorescence spectrometer by the crystal powders of the title MOF. The temperature-dependent fluorescence emission were conducted on a temperature controller attached to a cryostat (Oxford Ltd. Optistat DN2) on above fluorescence spectrometer. The angle-dependent fluorescence spectra were recorded by rotating a circular polarizer with scale from 0 to 330°. The polarizer was placed between the detector and the sample. The morphology of the MOF powders was investigated by using a field emission scanning electron microscope (SEM Sigma 500).

Optoelectronic properties tests were conducted by a CHI 660E electrochemical workstation. Using **1**-modified indium tin oxide (ITO) electrode with a working area

of 1.0 cm^2 as working electrodes, Ag/AgCl and platinum wire as reference and counter electrodes and 0.5 M Na_2SO_4 solution as the electrolyte. The three-electrode system was conducted in a quartz glass reactor ca. 50 cm^3 and irradiated by a 300 W xenon lamp. The cyclic voltammograms (CV) was performed with a scan rate of 50 mV/s. Transient photocurrent responses were tested through the on-off illumination at room temperature. Electrochemical impedance spectroscopy (EIS) Nyquist plots was obtained at the potential of 0 V and -0.5 V potential in three-electrode system. The relationship between current density and excitation wavelength was recorded by using RPEC-D Photoelectrochemical Analyzer (Xi'an Remex Analyse Instrument Co., Ltd., Xi'an, China). The monochromatic light was produced from a 300 W Xe arc lamp equipped with a Omni-λ150 monochromator.

2. Syntheses of [Cd(DCPA)(DMF)]·(H_2O) (1)

A mixture of 9,10-di(p-carboxyphenyl)anthracene (H_2DCPA, 0.1 mmol, 41.8 mg), $Cd(NO_3)_2·9H_2O$ (0.2 mmol, 80.0 mg), DMF (6 mL) and 60 μl of 68% HNO_3 were put in a 20 mL Pyrex vial, keeping the temperature at 100 ºC for 48 h to yield yellow block crystals after a natural cooling process to room temperature. Then, the resulting mixture was isolated, washed several times with DMF and dried in air. IR (KBr pellet, cm^{-1}): 3430 m, 3070 w, 1647 s, 1579 s, 1531 s, 1384 s, 1275 w, 1179 m, 1010 w, 946 m, 855 m, 763 s, 706 s, 666 s, 493 m.

3. X-ray single crystal structure

Single-crystal X-ray diffraction data were gathered at room temperature (293 K) on an Oxford Diffraction SuperNova area-detector diffractometer equipped with Mo-Kα X-

ray source (λ = 0.71073 Å). The data reduction was treated by using CrysAlis Pro software.[1] The crystal structure was solved by SHELXS-2014 program.[2] Crystallographic data of **1** was listed in Table S1. The CIF file of **1** (CCDC No. 2124068) can be gained free of charge via http://www.ccdc.cam.ac.uk/conts/retrieving.html.

4. Electronic structure calculations

The density functional theory (DFT) calculations were studied by Dmol3 in Material Studio software package.[3,4] The initial configuration was completely improved by Perdew-Wang (PW9**1**) generalized gradient approximation (GGA) way with the double numerical basis sets plus polarization function (DNP).[5] The core electrons for metals were dealt with effective core potentials (ECP).

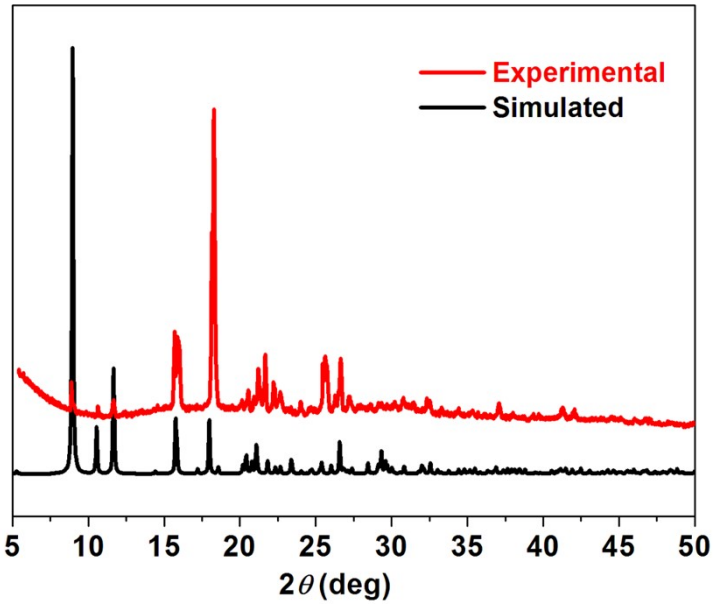

Figure S1. PXRD patterns of **1**.

Table S1. Crystallographic data for **1**.

Sample	[Cd(DCPA)(DMF)]·(H_2O) (**1**)
Chemical formula	$C_{31}H_{25}NCdO_6$
Formula weight	619.92
Crystal system	Monoclinic
Space group	*I*2/*a*
a (Å)	7.6683(6)
b (Å)	10.3179(13)
c (Å)	33.709(2)
α (°)	90.00
β (°)	95.667(7)
γ (°)	90.00
V (Å^3)	2654.0(4)
Z	4
D (g cm^{-3})	1.551
μ (mm^{-1})	0.869
R_{int}	0.0615
Goof	1.061
R_1[a] (*I*>2*σ* (*I*))	0.0674
wR_2[b] (*I*>2*σ*(*I*))	0.1257

[a] $R_1 = \Sigma(||F_o| - |F_c||)/\Sigma|F_o|$; [b] $wR_2 = [\Sigma w(|F_o|^2 - |F_c|^2)^2/\Sigma w(F_o^2)^2]^{1/2}$

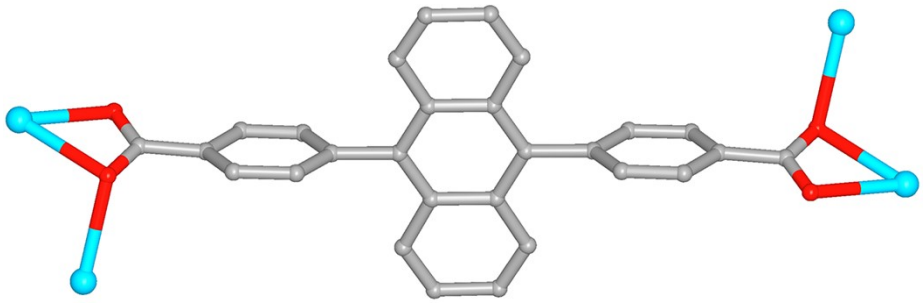

Figure S2. View of the coordination mode of DCPA in **1**.

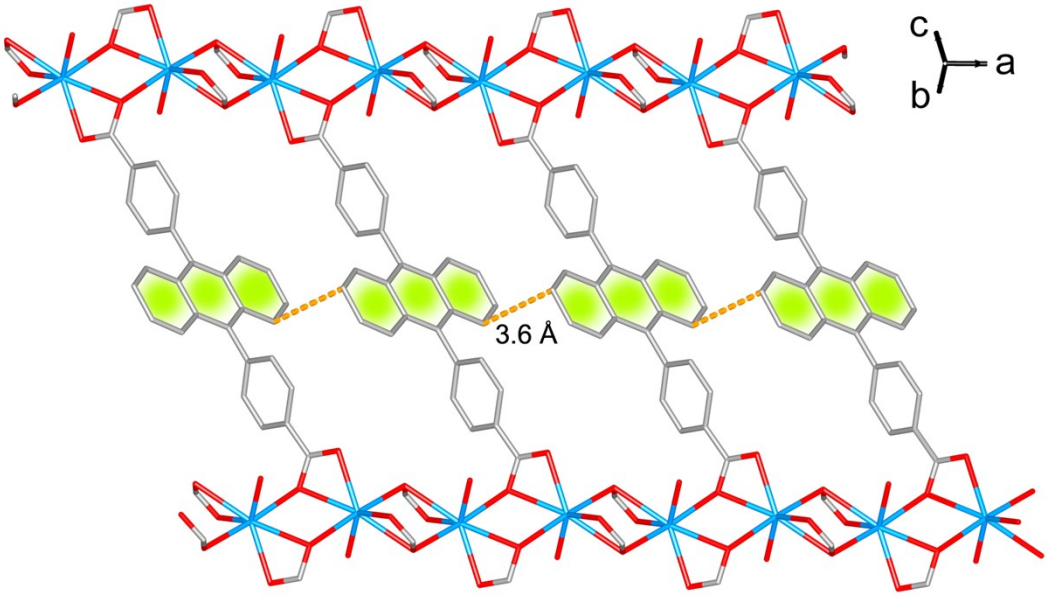

Figure S3. View of the parallel stacking of anthracene cores with the inter-plan distance of 3.6 Å arrange in **1**.

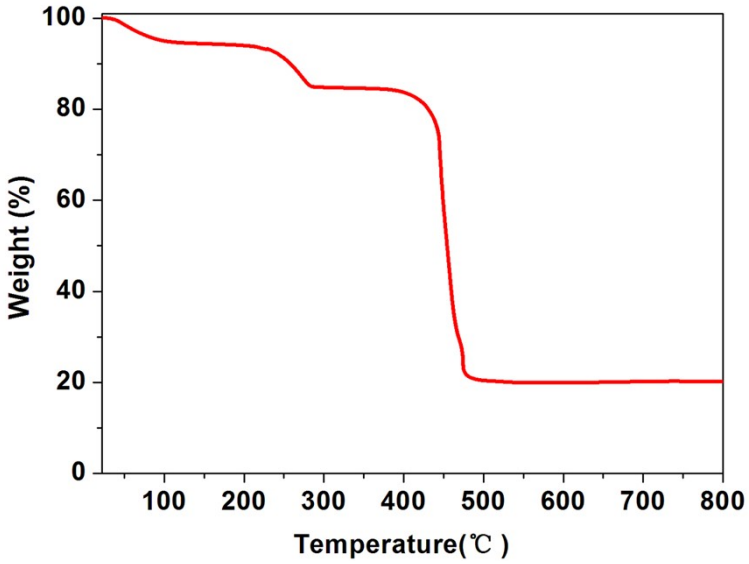

(a)

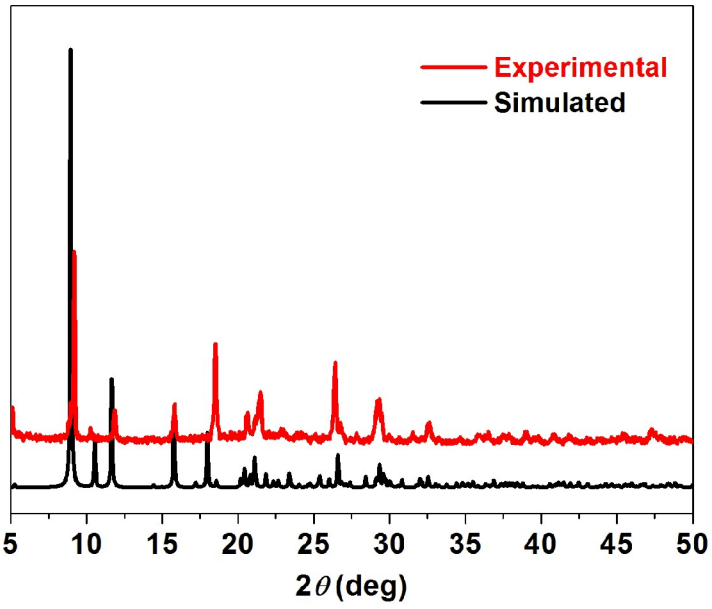

(b)

Figure S4. (a) Thermo gravimetric analysis (TGA) curve of **1**. (b) PXRD patterns of **1** after heating at 400 °C.

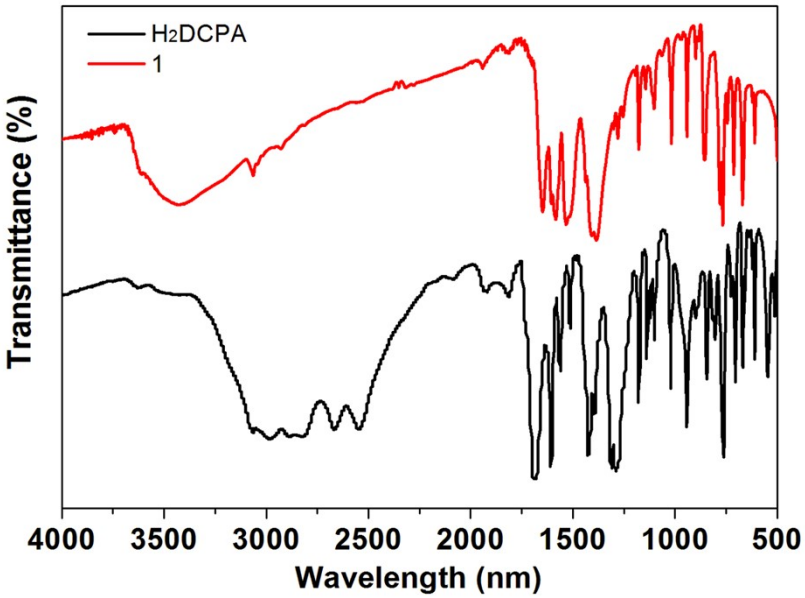

Figure S5. FT-IR spectra of free H_2DCPA ligand and **1**.

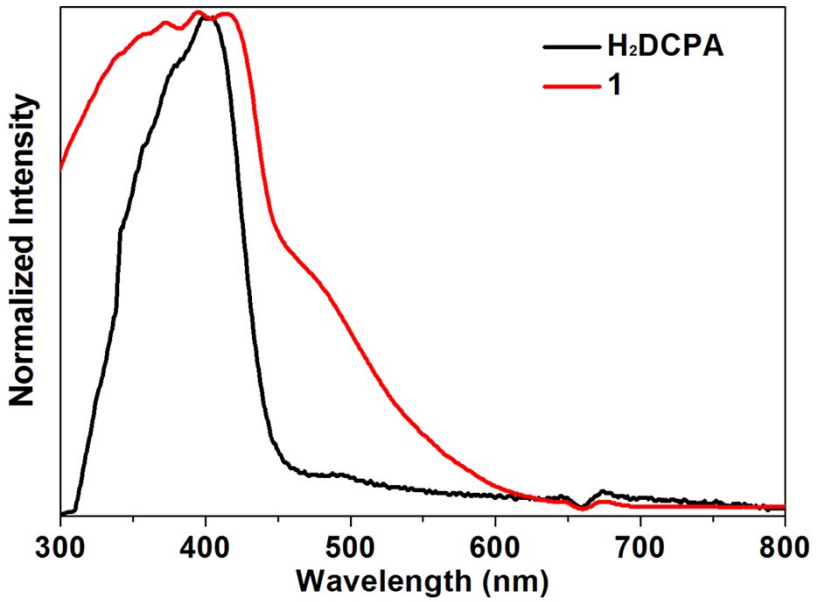

Figure S6. The UV-vis absorption curves of free H_2DCPA and **1** in solid state.

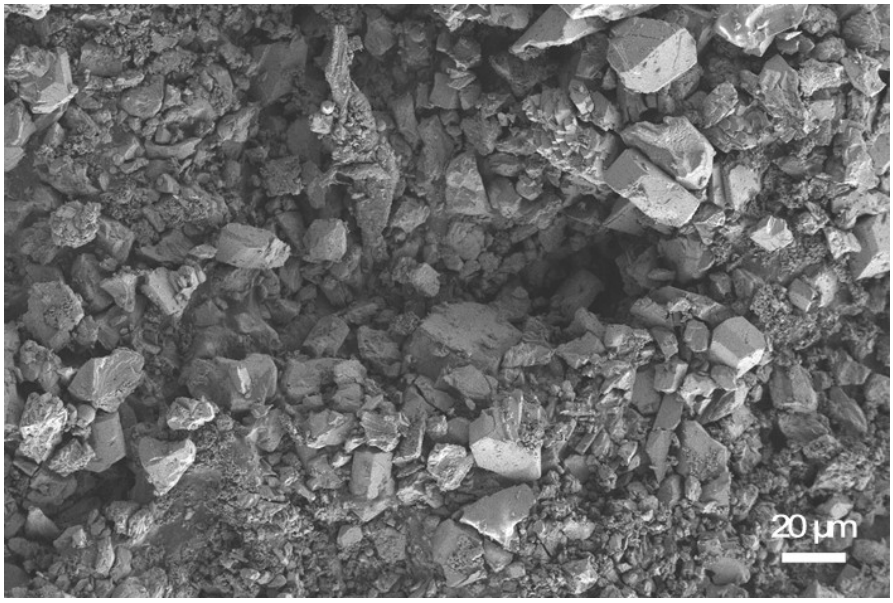

Figure S7. The SEM image of the powder of **1**.

Table S2. CIE-1931 chromaticity diagram for the temperature-dependent fluorescent emission

Temperature (K)	CIE (x,y)	Emission peak (nm)
73	0.1806,0.2191	459
93	0.1829,0.2310	462
113	0.1849,0.2412	465
133	0.1866,0.2498	467
153	0.1891,0.2614	471
173	0.1916,0.2716	473
193	0.1947,0.2840	477
213	0.1984,0.2972	479
233	0.2018,0.3080	482
253	0.2063,0.3182	485
273	0.2103,0.3262	487
293	0.2132,0.3331	490

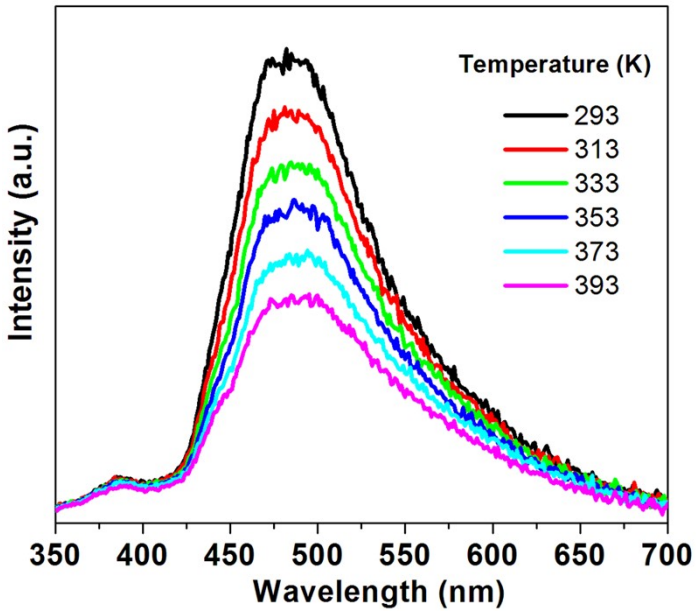

(a)

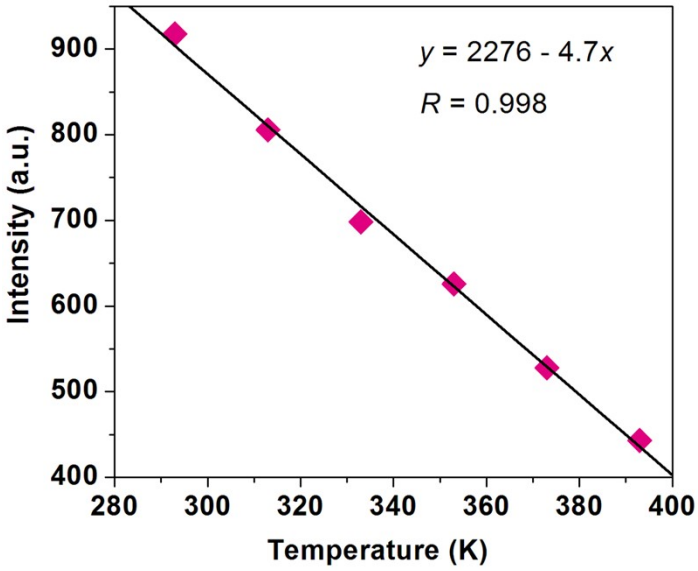

(b)

Figure S8. (a) Fluorescence spectra of **1** recorded in the temperature range of 293-393 K excited at 330 nm. (b) Temperature-dependent maximum fluorescence intensity and fitted curve in the temperature range of 293-393 K.

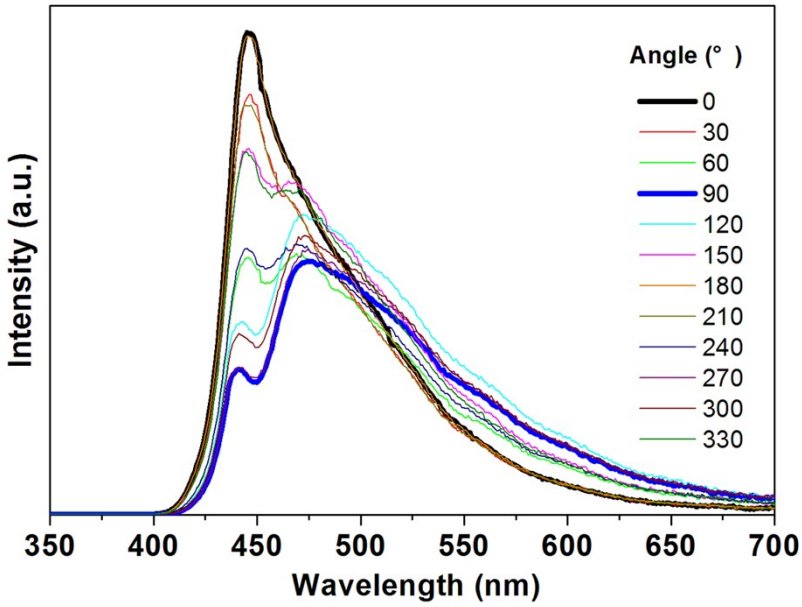

Figure S9. Angle-dependent polarized fluorescence spectra of **1** measured from 0 to 330°.

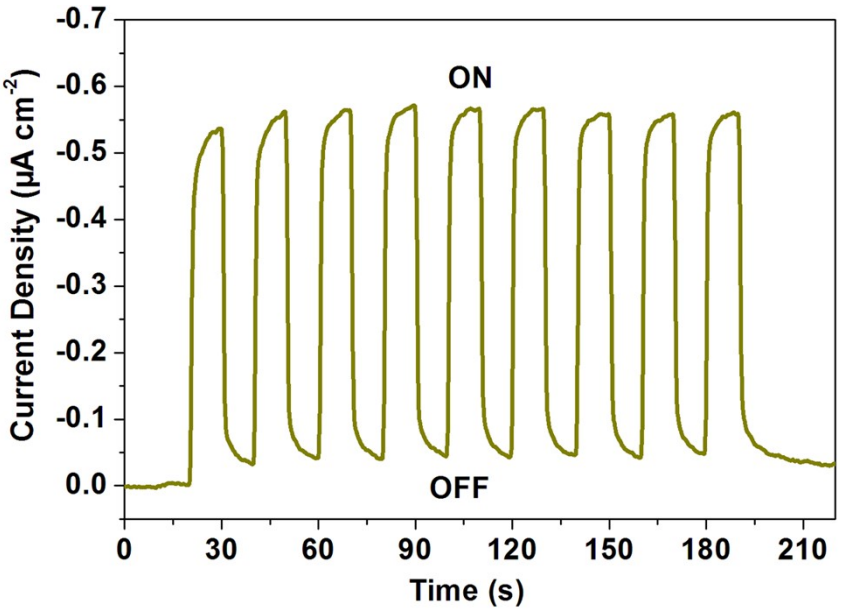

(a)

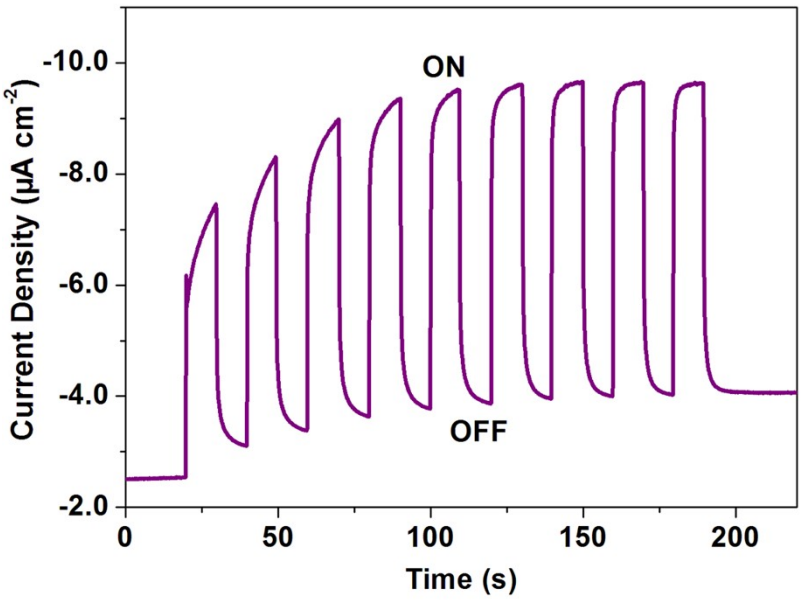

(b)

Figure S10. Transient current density–time curves of **1** measured under the bias potential of 0 (a) and -0.5 V (b).

Supporting References

1. CrysAlisPro, Rigaku Oxford Diffraction, Version 1.171.39.6a.
2. G. M. Sheldrick, *Acta Crystallogr. Sect. A* 2008, **64**, 112.
3. (*a*) B. Delley, *J. Chem. Phys*. 1990, **92**, 508; (*b*) B. Delley, *J. Chem. Phys*. 2000, **113**, 7756.
4. Dmol3 Module, MS Modeling, Version 2.2; Accelrys Inc.: San, Diego, 2003.
5. J. P. Perdew, J. A. Chevary, S. H. Vosko, K. A. Jackson, M. R. Pederson, D. J. Singh and C. Fiolhais, *Phys. Rev. B* 1992, **46**, 6671.